

RESEARCH ARTICLE | MAY 13 2024

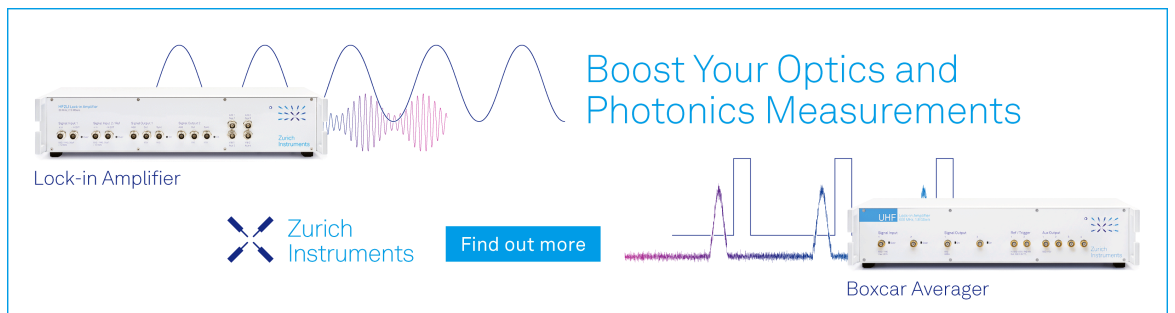
Weak signal detection technique based on Durbin–Watson test and one-bit sampling

Xiru Zhao ; Jiadong Hu  ; Kenan Wu ; Haiyun Xia ; Daihao Yu 



Rev. Sci. Instrum. 95, 054705 (2024)

<https://doi.org/10.1063/5.0198084>



Boost Your Optics and Photonics Measurements

Lock-in Amplifier

Zurich Instruments

Find out more

Boxcar Averager

Weak signal detection technique based on Durbin–Watson test and one-bit sampling

Cite as: *Rev. Sci. Instrum.* **95**, 054705 (2024); doi: [10.1063/5.0198084](https://doi.org/10.1063/5.0198084)

Submitted: 16 January 2024 • Accepted: 24 April 2024 •

Published Online: 13 May 2024



View Online



Export Citation



CrossMark

Xiru Zhao,¹ Jiadong Hu,^{1,a)} Kenan Wu,^{1,2} Haiyun Xia,^{1,2,3} and Daihao Yu¹

AFFILIATIONS

¹China Meteorological Administration Aerosol-Cloud and Precipitation Key Laboratory, School of Atmospheric Physics, Nanjing University of Information Science and Technology, Nanjing 210044, China

²School of Earth and Space Science, University of Science and Technology of China, Hefei 230026, China

³National Laboratory for Physical Sciences at the Microscale, University of Science and Technology of China, Hefei 230026, China

^{a)}Author to whom correspondence should be addressed: hujd0707@nuist.edu.cn

ABSTRACT

Correlation-based detection techniques are widely used in the weak periodic signal detection field. Traditionally, they are based on extracting the correlation of a weak signal from noise. Considering the impact of a weak signal on the randomness of background noise, this article takes the opposite approach and proposes a weak signal detection technique based on the Durbin–Watson (DW) test and one-bit sampling, detecting the weak signal due to the extent to which the randomness of noise is affected. The randomness of noise is analyzed through the DW test, which is a method for detecting the randomness of data sequences through first-order autocorrelation. One-bit sampling is adopted to reduce the complexity of the sampling circuit and data processing algorithm. The effectiveness of the DW test in the situation of one-bit sampling is demonstrated through simulation and analysis. Simulation results show that the proposed technique is capable of detecting weak sinusoidal and square-wave signals with a signal-to-noise ratio (SNR) above -30 dB, and the frequency or SNR of a weak signal can be further estimated based on mutual constraints. The measured results confirm the capability. In addition, the factors of coherent sampling, noise bandwidth, and comparator threshold that influence the performance of the proposed technique are simulated and discussed in detail.

Published under an exclusive license by AIP Publishing. <https://doi.org/10.1063/5.0198084>

I. INTRODUCTION

A weak signal refers to a signal that is overwhelmed by strong noise,^{1,2} and corresponding detection techniques have been widely applied in radar,^{3–5} communication,^{6–8} wheelset-bearing fault detection,^{9–11} and other fields.

Over the years, various weak periodic signal detection techniques have been proposed and developed for different applications. Correlation-based detection is one of the earliest techniques proposed for weak signal detection.¹² In particular, correlation-based detection techniques mainly use the autocorrelation function and/or cross-correlation function to detect weak periodic signals from noise.^{13–15} The traditional methods extract the correlation coefficients of each order of the weak signal components in the mixed signal with noise. Based on the characteristics of the correlation coefficients, the presence or absence of the weak signal is determined, i.e., the weak signal is detected according to

the correlation function of the weak signal. It is worth noting that the well-known instrument called a lock-in amplifier is a typical example that uses the cross-correlation function to detect weak signals.^{16–18}

Many alternative weak signal detection techniques have also been extensively developed, including coherent integration,^{2,19,20} stochastic resonance,^{21–23} chaotic oscillators,^{24–26} and wavelet transforms.^{27–29} Coherent integration is a simple but effective technique for weak signal detection. The signal can be coherently integrated in the time or frequency domain, as the energy increase speed of the weak signal component is faster than that of the noise component. The more times the signal is coherently integrated, the higher signal-to-noise ratio (SNR) will be achieved until the weak signal is detected. Benzi *et al.* initially proposed the concept of stochastic resonance in 1981 to explain the periodic alternation of glacial and warm climates in paleometeorology;^{30–32} later, the idea of stochastic resonance was introduced into the field of weak signal detection in the 1990s. Stochastic resonance is a unique technique

that uses noise for weak signal detection, rather than suppressing noise. In a constructed bistable system that is driven by a weak signal, the noise is utilized for steady-state switching. The seemingly random pulse output from the bistable system can be analyzed through the spectrum or pulse interval to judge the presence of a weak signal.^{11,33} The chaotic oscillator is a distinctive weak signal detection technique based on the theory of chaos. By adjusting parameters, a nonlinear system is placed in a critical, chaotic state. When the system receives a weak signal of a specific frequency, the phase diagram will convert from a chaotic state to a great period state; thus, the presence of a weak signal can be determined. However, the parameters of the system are closely related to the characteristics of weak signals; experience in parameter adjustment is required, and no fixed pattern can be followed.³⁴ The wavelet transform is a time-frequency analysis technique that shares similarities with the fast Fourier transform but is distinct from it. Compared to the fast Fourier transform, the wavelet transform excels at extracting weak signals from noise. However, the selection of wavelet basis functions is quite difficult. As with the chaotic oscillator technique, there is no standard or generic method for wavelet basis function selection.¹

The idea of weak signal detection techniques based on the correlation of weak signals inspired the use of the opposite technique in this article. Since the weak signal is mixed with strong noise, the mixed signal not only has weaker autocorrelation than the weak signal component but also has weaker randomness than the noise component. Therefore, techniques for testing the randomness of the noise can also be used to detect weak signals, according to the reduction of randomness after the weak signal is added to the noise.

The Durbin–Watson (DW) test is widely utilized to assess the randomness of noise using a simple statistic based on the first-order autocorrelation coefficient.^{35–37} Other alternative methods include the Breusch–Godfrey test,^{37,38} the Ljung–Box test,^{39,40} etc. The Breusch–Godfrey test functions by regressing the residuals of a time series model on the lagged values of those residuals and examining the significance of those lagged residuals, while the significance indicates randomness. The Ljung–Box test statistic is calculated by examining the sum of squares of autocorrelations at different lags in the time series. Again, the significance of the test statistic indicates randomness. In this article, the DW test is adopted for performing the randomness test of noise. Since the detection of weak signals usually necessitates a significant amount of data for computation, in order to reduce the computational complexity of the DW test and make it easier to implement in the hardware, the noise data for the DW test is attempted to be sampled using a one-bit analog-to-digital converter (ADC).

This article proposes a weak signal detection technique based on the DW test and one-bit sampling, adopts an easy-to-implement one-bit ADC that is realized through a comparator (CMP) and a shift register (SR),^{2,41} and optimizes the implementation of the DW test to fit one-bit sampling. The result of the DW test reflects whether a weak signal exists or not and can be further used to estimate the frequency, or SNR, of the weak signal. The effect of weak sinusoidal and square-wave signals on the randomness of white Gaussian noise (WGN) is simulated, and the simulation results show that the proposed technique is able to detect weak signals from WGN in situations of SNR above -30 dB. The interferences

of coherent sampling, noise bandwidth, and comparator threshold on the proposed technique are discussed. Further experimental results verify the effectiveness of the proposed weak signal detection technique.

The rest of the article is organized as follows: Sec. II details the proposed weak signal detection technique based on the DW test and one-bit sampling, Sec. III illustrates the test results with a prototype based on the proposed technique, and Sec. IV concludes the article.

II. PROPOSED TECHNIQUE

Figure 1 shows the architecture of the proposed weak signal detection technique based on the DW test and one-bit sampling. The mixed signal, which consists of weak signal and noise, is compared with a threshold voltage (TH) through a CMP. The output of the CMP, which is a two-level signal, is sent to a field programmable gate array (FPGA) and sampled into one-bit data by SRs in multiple channels. Each SR is composed of several cascaded flip flops. The CMP and SR equivalently form a one-bit ADC.^{2,41} The delay units (DUs) are used to regulate the time offset of a two-level signal in each channel so that the sampling point of each channel is at a different time. This design enables randomness testing to be conducted in parallel across multiple channels. In the DW test module (DWTM), the deviation degree of DW statistics between the mixed signal and the WGN is calculated in each DW error unit (DWEU). An average (AVG) unit is used to provide the average of one-bit data for the DWEUs. The mean value of the DW errors is then calculated and output. This value indicates the randomness of the mixed signal.

Using a CMP and SRs to obtain multi-channel, one-bit data reduces the implementation complexity of the sampling circuit and the computational complexity of the DW test while preserving the randomness of the mixed signal. In addition, multi-channel parallel

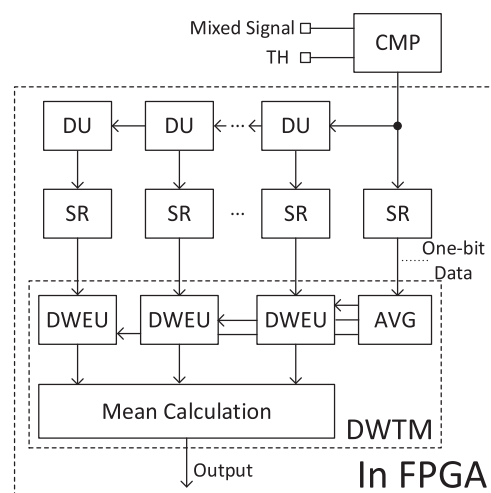


FIG. 1. Architecture of the proposed weak signal detection technique based on the DW test and one-bit sampling.

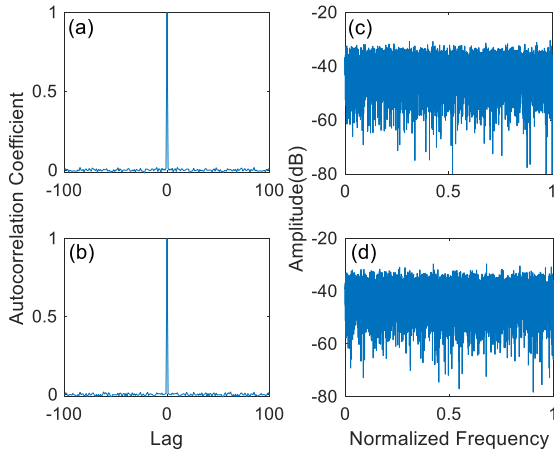


FIG. 2. Autocorrelation functions and power spectra of sampled WGN data: (a) autocorrelation function of WGN sampled by a 16-bit ADC, (b) autocorrelation function of WGN sampled by a one-bit ADC, (c) power spectrum of WGN sampled by a 16-bit ADC, and (d) power spectrum of WGN sampled by a one-bit ADC.

computing reduces the data processing time, making the DWTM easy to process the one-bit data in real-time.

A. One-bit sampling of mixed signals

The mixed analog signal can be sampled for randomness analysis. Conventionally, an analog signal to be analyzed is sampled by a high-resolution ADC and then processed through hardware or software based digital signal processing techniques. However, for weak signals submerged in strong noise, the sampling waveform inevitably has significant distortion, so the resolution of the ADC can be reduced to the limit of one-bit to decrease the computational complexity. Nevertheless, the impact of one-bit sampling on the randomness of mixed signals needs to be confirmed. Figure 2 shows the autocorrelation functions and power spectra of WGN, sampled by a 16-bit ADC and by a one-bit ADC. It can be seen that after reducing the resolution of the ADC from 16-bits to one-bit, the randomness of the WGN is still effectively inherited by the sampled data. Therefore, using a one-bit ADC to sample the mixed signal and conducting a subsequent randomness analysis is feasible. Moreover, reducing the bit-width of the data will assist in decreasing the computational complexity of the DW test.

To implement a one-bit ADC, either an ADC chip or a one-bit ADC composed of a CMP and a SR can be used.^{2,41} The CMP and SRs based method simplifies the design of the circuit and is, therefore, used in this article.

B. DW test based on one-bit data

As a typical method for detecting randomness of noise, the DW test condenses the correlation information of a data sequence into a concise number, i.e., the DW statistic. This method is essentially based on the first-order autocorrelation coefficient of the data sequence.^{35–37}

Assuming that the one-bit data sequence of noise contains n data points. The DW statistic is defined as³⁵

$$DW = \frac{\sum_{k=2}^n (e_k - e_{k-1})^2}{\sum_{k=1}^n e_k^2}, \quad (1)$$

where e_k denotes the residual of the k -th one-bit data ($k = 1, 2, \dots, n$),

$$e_k = d_k - \bar{d}, \quad (2)$$

where d_k refers to the k -th one-bit data, and \bar{d} represents the mean value of the one-bit data sequence. As a comparison, the first-order autocorrelation coefficient is defined as⁴²

$$\rho = \frac{\sum_{k=2}^n e_k e_{k-1}}{\sum_{k=1}^n e_{k-1}^2}, \quad (3)$$

which means

$$DW \approx 2(1 - \rho). \quad (4)$$

As can be seen, if the one-bit data show randomness, the value of ρ will tend to 0, and the DW statistic will tend to 2.⁴²

The WGN is completely random and has no autocorrelation; therefore, its DW statistic is approximately equal to 2. However, the introduction of the weak signal disturbs the randomness of WGN, resulting in the mixed signal having a first or higher order autocorrelation. The manifestation is that the DW statistic deviates to some extent from 2. Thus, it is feasible to identify the presence of a weak signal and estimate its SNR by analyzing the degree of deviation from 2 of the DW statistics.

In the case of one-bit sampling, the calculation of the DW statistic can be simplified. For the numerator part in Eq. (1), there is

$$\begin{aligned} (e_k - e_{k-1})^2 &= (d_k - d_{k-1})^2 \\ &= \begin{cases} 1, & d_k \neq d_{k-1} \\ 0, & d_k = d_{k-1} \end{cases} \\ &= d_k \oplus d_{k-1}. \end{aligned} \quad (5)$$

Where $x \oplus y$ means an XOR operation between x and y , easy to implement in hardware. In addition, as there is $d_k^2 = d_k$ in one-bit sampling, the denominator part in Eq. (1) can be simplified as

$$\begin{aligned} \sum_{k=1}^n e_k^2 &= \sum_{k=1}^n (d_k - \bar{d})^2 \\ &= \sum_{k=1}^n d_k^2 + \sum_{k=1}^n \bar{d}^2 - 2\bar{d} \sum_{k=1}^n d_k \\ &= n\bar{d} + n\bar{d}^2 - 2n\bar{d}^2 \\ &= n\bar{d}(1 - \bar{d}). \end{aligned} \quad (6)$$

As a result, the value of $\sum_{k=1}^n e_k^2$ can be simply obtained by calculating the average value of d_k , i.e., \bar{d} . The reduction of computational complexity facilitates the high speed and real-time implementation in the hardware of the DW test.

In order to describe the extent to which the randomness of the noise is affected by the weak signal, an index is defined as

$$DWE = 2 - DW. \quad (7)$$

It is obvious that

$$DWE \approx 2\rho, \quad (8)$$

i.e., DWE represents the first-order autocorrelation of the noise. When the weak signal has a detectable SNR, the DWE will deviate from 0 and provide information for SNR estimation.

C. Simulation of the proposed technique

It is evident from Eq. (8) that there is a linear relationship between the DWE and the first-order autocorrelation coefficient for the mixed signal. Since there should be a linear relationship between the first-order autocorrelation coefficient of the mixed signal and the power of the weak signal, there should also be a linear relationship between the DWE of the mixed signal and the power of the weak signal. As the SNR of a weak signal is linearly related to the logarithm of its power, it can be expected that $\lg(DWE)$ will exhibit a linear relationship with SNR.

To verify the relationship between the SNR and DWE, simulations using MATLAB were carried out on a mixed signal that contains WGN and a weak sinusoidal or square-wave signal. The sampling rate of the one-bit ADC was normalized to 1, and the normalized repetition rate of the weak signal was within 0.5, i.e., within the first Nyquist band. The mixed signal was compared to TH, which was set to the mean value of WGN. The generated one-bit data were used to calculate the DWE, with a data length of 2.¹⁸ The absolute value of the mean of the DWE (DWEM) was obtained by averaging 10 000 DWEs and then taking the absolute value.

The detection of weak sinusoidal signals was simulated in detail. The normalized frequencies of the weak sinusoidal signals were 0.1, 0.2, 0.25, 0.3, and 0.4. The SNRs of the weak signals ranged from -40 to 5 dB, with a step of 1 dB. The simulation results are shown in Fig. 3. For sinusoidal signals with frequencies of 0.1, 0.2, 0.3, and 0.4, the relationship between $\lg(DWEM)$ and SNR shows the expected linearity with the same slope of 0.1. Due to this, when the SNR of a weak sinusoidal signal is above -30 dB, the weak sinusoidal signal is detectable, and the SNR or frequency can be evaluated through the relationship between DWEM, frequency, and SNR.

The relationship between DWEM, frequency, and SNR in Fig. 3 can be written as follows:

$$\begin{aligned} \log_{10}(DWEM(Fre, SNR)) \\ = \log_{10}(SIN_DWEM_0(Fre)) + 0.1 \times SNR, \end{aligned} \quad (9)$$

or

$$DWEM(Fre, SNR) = SIN_DWEM_0(Fre) \times 10^{0.1 \times SNR}, \quad (10)$$

where Fre denotes the frequency of the weak sinusoidal signal, and SIN_DWEM_0 refers to the DWEM value when the SNR of a weak

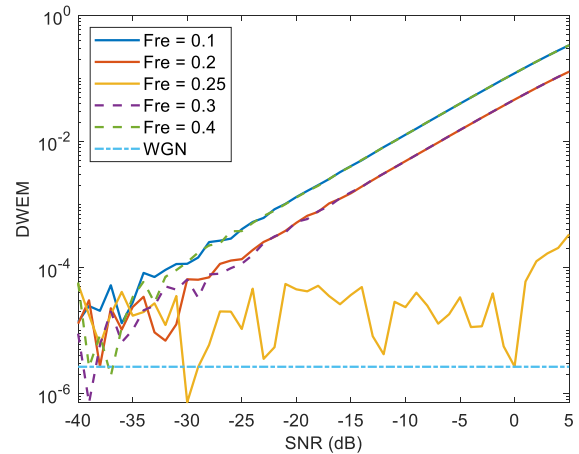


FIG. 3. DWEM vs SNR of a weak sinusoidal signal at different frequencies.

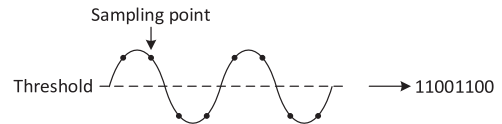


FIG. 4. Diagram of using a one-bit ADC to sample a sinusoidal signal at the normalized frequency of 0.25.

sinusoidal signal is 0 dB and is correlated with the weak sinusoidal signal frequency.

It is worth noting that, as shown in Fig. 3, the proposed technique encounters difficulty in detecting a weak sinusoidal signal at a frequency of 0.25. Further study reveals that, as shown in Fig. 4, it is because when the weak sinusoidal signal of this frequency is sampled, the one-bit sampled data happens to have second-order autocorrelation and minimal first-order autocorrelation. Therefore, due to one-bit sampling, the DW test, which is based on first-order autocorrelation, cannot effectively detect weak sinusoidal signals at a frequency of 0.25, even if the SNR is large.

In addition, it can be seen in Fig. 3 that a weak sinusoidal signal with a frequency of 0.1 behaves almost identically to a weak sinusoidal signal with a frequency of 0.4, and this is also the case at the frequencies of 0.2 and 0.3. To clarify the relationship between DWEM and the frequency of the weak sinusoidal signal, DWEM vs the frequency of the weak sinusoidal signal was simulated. The SNR was 0 dB, and the frequency varied from 0.01 to 0.49, with a step of 0.01. The simulation result is shown in Fig. 5. It can be seen that the curve is symmetrical around the frequency of 0.25, consistent with the results shown in Fig. 3.

Furthermore, the curve in Fig. 5 can be well fitted using quadratic functions. When $0 < Fre < 0.25$, the DWEM corresponds to the weak sinusoidal signal at an SNR of 0 dB is

$$SIN_DWEM_0(Fre) = -1.3844(Fre)^2 - 0.3226Fre + 0.1683, \quad (11)$$

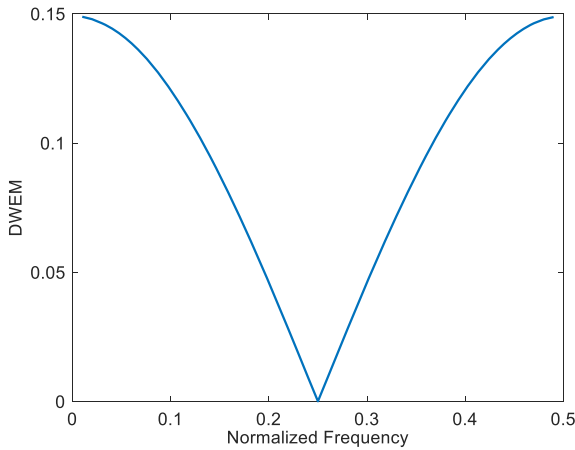


FIG. 5. DWEM vs frequency of a weak sinusoidal signal when SNR is 0 dB.

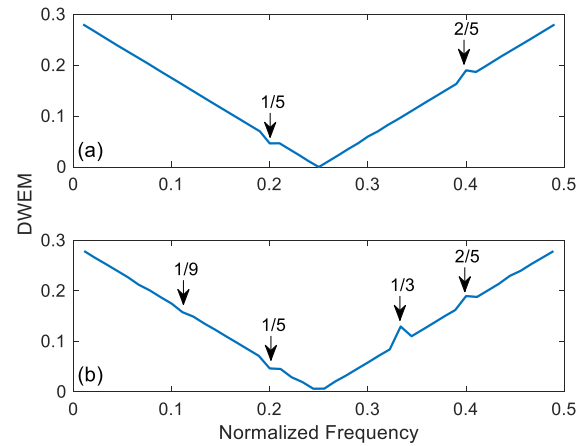


FIG. 7. DWEM vs frequency of a weak square-wave signal when SNR is 0 dB. (a) Simulation frequency interval is 1/100, and (b) simulation frequency interval is 1/90.

and when $0.25 < Fre < 0.5$, the equation can be written as

$$SIN_DWEM_0(Fre) = -1.3844(0.5 - Fre)^2 - 0.3226(0.5 - Fre) + 0.1683 \quad (12)$$

In the situation of undersampling, Eqs. (11) and (12) are still effective, except that the frequency should be folded into the first Nyquist band.

The detection of weak square-wave signals was also simulated in detail. The simulation conditions for DWEM vs SNR were identical to those for weak sinusoidal signals in Fig. 3, with the exception that square-wave signals were used instead of sinusoidal signals. The simulation result is shown in Fig. 6. Compared to Fig. 3, the curves of frequency at 0.1 and 0.4 are not coincident, and the curves of frequency at 0.2 and 0.3 are not coincident either. The curve of frequency at 0.25 maintains its characteristics.

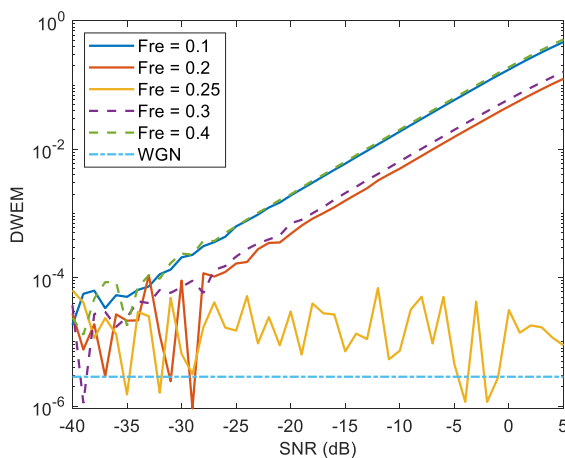


FIG. 6. DWEM vs SNR of a weak square-wave signal at different frequencies.

The reason for noncoincidence was further studied through simulation. The relationship between DWEM and the frequency of a weak square-wave signal was simulated. The SNR was 0 dB, and the frequency swept in two directions: from 1/100 to 49/100 with a step of 1/100, and from 1/90 to 44/90 with a step of 1/90. Figure 7 shows that the deviations from the expected values occur at the frequencies of 1/9, 1/5, 1/3, and 2/5, which meet the coherent sampling condition. This reveals the impact of coherent sampling on DWEM when the weak signal under detection is a square-wave.

When the frequency of the weak square-wave signal is 0.25, the one-bit sampled data of the square-wave signal resembles the sinusoidal signal shown in Fig. 4, which mainly contains second-order autocorrelation. Therefore, in Fig. 7, the DWEM value at the frequency of 0.25 is also close to 0, similar to the situation in Fig. 5.

The impact of coherent sampling on DWEM is further studied for weak square-wave signal detection. In cases of coherent sampling, due to the certainty of sampling position in the waveform period, the first-order autocorrelation is enhanced for the high-frequency square-wave signal. Similarly, for the low-frequency square-wave signal, the high-order autocorrelation is strengthened, which means the first-order autocorrelation is weakened. For example, when a square-wave signal at a frequency of 1/5 is coherently sampled, as shown in Fig. 8(a), the one-bit data are a repetition of 11 000 or 00 111, which mainly contains high-order autocorrelation, resulting in a smaller than expected DWEM in Fig. 7. At the frequency of 2/5, as shown in Fig. 8(b), the one-bit data are a repetition of 11 010 or 00 101, which contains strong first-order autocorrelation, resulting in a larger than expected DWEM in Fig. 7. However, by sampling the same signal with three coprime sampling rates and taking two of the closer DWEM results as valid results, the impact of coherent sampling can be eliminated, as the coherent sampling occurs between at most one sampling rate and the weak square-wave signal.

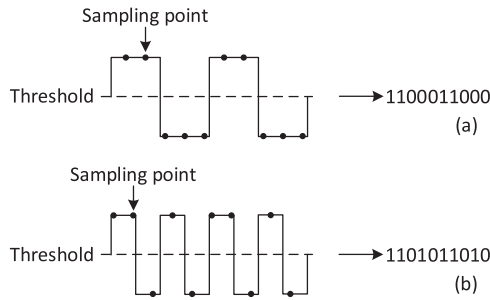


FIG. 8. Diagram of using a one-bit ADC to sample a square-wave signal at the normalized frequency of (a) 1/5 and (b) 2/5.

After removing the coherent sampling points, the curve in Fig. 7 can be well fitted as a linear curve composed of two segments. When $0 < Fre < 0.25$, the DWEM corresponds to the weak square-wave signal at 0 dB is

$$SQ_DWEM_0(Fre) = -1.1709Fre + 0.2920, \quad (13)$$

when $0.25 < Fre < 0.5$,

$$SQ_DWEM_0(Fre) = -1.1709(0.5 - Fre) + 0.2920, \quad (14)$$

where SQ_DWEM_0 represents the DWEM value of a weak square-wave signal when SNR is 0 dB. In the situation of undersampling, Eqs. (13) and (14) are still effective, except that the frequency should be folded into the first Nyquist band. In addition, the relationship between DWEM, Fre , and SNR can also be described as Eqs. (9) and (10), except that the SIN_DWEM_0 should be replaced by SQ_DWEM_0 .

Based on the simulations and analysis, the proposed technique can be used to detect weak sinusoidal or square-wave signals. The relationship between DWEM, Fre , and SNR further enables the estimation of SNR or frequency for these two kinds of weak signals.

D. Interferences of noise bandwidth and CMP threshold

In practical applications, the noise has a limited bandwidth, and normally the threshold of CMP is not the same as the mean value of noise. This may influence the performance of the proposed weak signal detection technique. The interference from them was simulated. In the simulation of noise bandwidth interference, the sampling rate of the one-bit ADC was normalized to 1, and the TH was set to be equal to the mean value of noise. A WGN was filtered through a first-order Butterworth filter to generate noise with limited bandwidth; the bandwidth ranged from 0.5 to 1.5 with an increment of 0.005. The simulation result of DWEM of noise vs noise bandwidth is shown in Fig. 9. It is evident that a linear relationship exists between the $\lg(DWEM_{noise})$ and the bandwidth of the noise, which can be described as

$$DWEM_{noise} = 10^{-2.717 \times BW + 0.1256}, \quad (15)$$

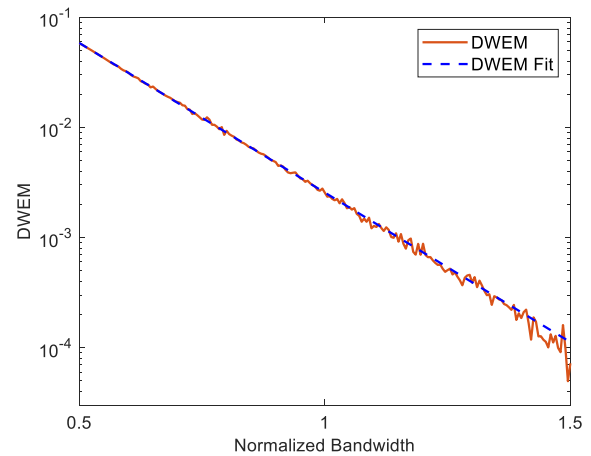


FIG. 9. DWEM of noise vs noise bandwidth when the ADC sampling rate is normalized to 1.

where BW denotes the ratio of the noise bandwidth to the ADC sampling rate.

In Figs. 3 and 6, it can be seen that the proposed weak signal detection technique requires the DWEM of the noise component to not reach the same level as the DWEM of the weak signal mixed with WGN. According to Eq. (15), this means the ratio of the noise bandwidth to the ADC sampling rate should be large enough. Fortunately, the interference of the noise bandwidth can be overcome by reducing the ADC sampling rate when the noise bandwidth cannot be increased.

The following is a simulation of the interference of the CMP threshold with weak sinusoidal and square-wave signals. The sampling rate of one-bit ADC was normalized to 1, and the frequency of the weak signal was 0.21. The weak signal was mixed with WGN, and the standard deviation of WGN was set to 1. The THs ranged from -5 to 5 with a step of 0.1, and the SNRs of the weak signals

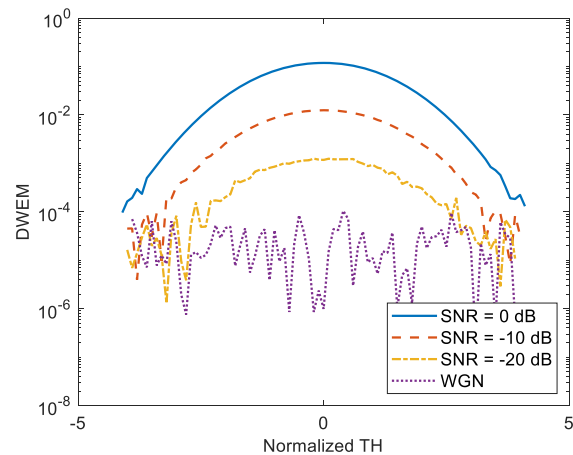


FIG. 10. DWEM vs TH of CMP in weak sinusoidal signal detection.

TABLE I. Impact of the variation range of TH on DWEM in weak sinusoidal signal detection when the signal frequency is 0.21 and the SNR is 0 dB.

Δ TH	Δ DWEM (%)
± 0.1	0.41
± 0.2	1.49
± 0.5	8.94
± 1	31.57

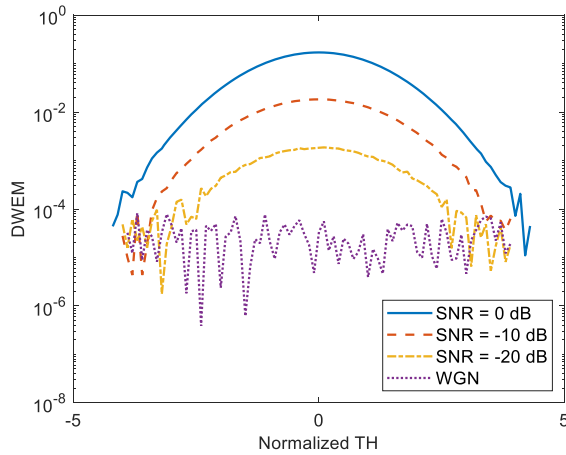


FIG. 11. DWEM vs TH of CMP in weak square-wave signal detection.

varied from -20 to 0 dB with a step of 10 dB. The simulation result of DWEM vs TH of CMP in weak sinusoidal signal detection is shown in Fig. 10. It can be seen that the interference of TH on the DWEM of a weak sinusoidal signal increases as the SNR increases. When the TH is greater than 4 or less than -4 , the one-bit data will be almost all 0 s or all 1 s, causing the DW to be unable to calculate and rendering the detection technique ineffective. Typically, when the SNR of a weak sinusoidal signal is 0 dB, the impact of the variation range of TH on DWEM is shown in Table I. For different detection accuracy requirements, the range requirement of TH can be evaluated so that TH variations have a sufficiently small effect on weak sinusoidal signal detection.

Figure 11 shows the simulation results of DWEM vs TH of CMP in weak square-wave signal detection. Compared with Fig. 10, the simulation results of weak sinusoidal and square-wave signals

TABLE II. Impact of the variation range of TH on DWEM in weak square-wave signal detection when the signal frequency is 0.21 and the SNR is 0 dB.

Δ TH	Δ DWEM (%)
± 0.1	0.43
± 0.2	1.70
± 0.5	10.03
± 1	34.62

are quite similar. When the SNR of a weak square-wave signal is 0 dB, the impact of the variation range of TH on DWEM can be seen in Table II.

III. TEST RESULTS

A prototype was implemented to validate the proposed weak signal detection technique based on the DW test and one-bit sampling. Figure 12 displays the block diagram of the measurement system. The sinusoidal signal was generated by a Rohde & Schwarz RF signal source (SMB100A), the square-wave signal was generated by a Tektronix arbitrary waveform generator (AFG3102C), and the WGN with a bandwidth of 1.5 GHz was generated by a NoiseCom noise source (UFX7110B). To control the SNR of the weak signal, a step attenuator was utilized to attenuate the sinusoidal or square-wave signal. In the prototype, the CMP (TLV3604DCKR⁴³) was used for quantization, and flip flops on an FPGA chip (XC7K325T-2FFG900I⁴⁴) were used for sampling. The sampling rate was set at 5 mega samples/s (MSPs) to avoid interference with the bandwidth limit of WGN. The DW test results from the FPGA were then sent to a personal computer (PC) for SNR, or frequency estimation.

A test that uses the DWEM value to evaluate the SNR of the weak sinusoidal or square-wave signal was performed. The frequency of the weak signal was set to 600 kHz. The test result is shown in Fig. 13. It can be seen that the weak signal can be detected with the SNR above -30 dB. However, due to the non-ideal character of

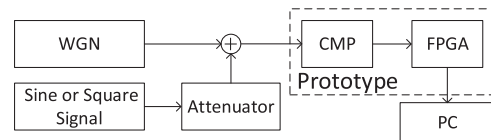


FIG. 12. Block diagram of the measurement system.

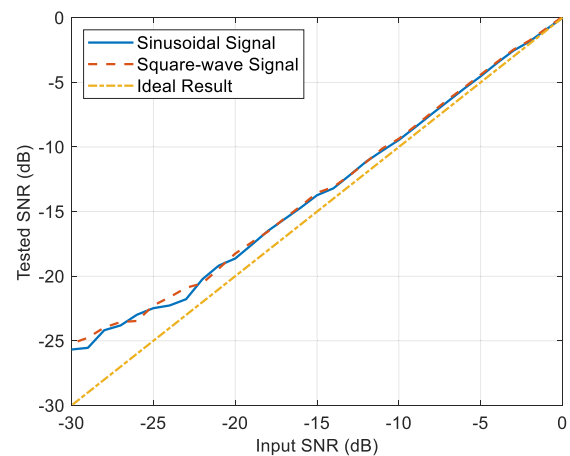


FIG. 13. Test results of SNR estimation with the weak signal frequency of 600 kHz and the sampling frequency of 5 MSPs.

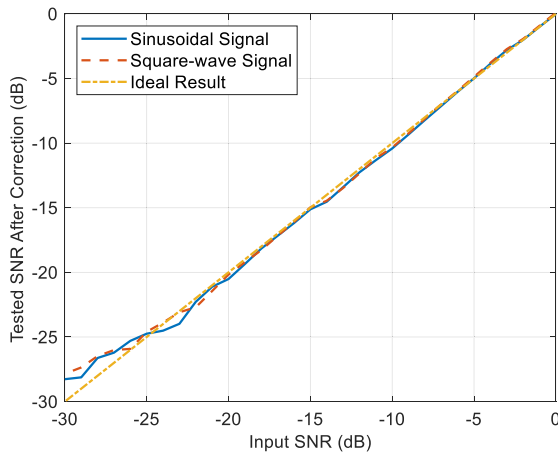


FIG. 14. Corrected test results of SNR estimation with the weak signal frequency of 600 kHz and the sampling frequency of 5 Msps.

the comparator and the deviation between the TH and noise mean value, the measured SNR may deviate from the theoretical expectations to some extent. The deviation can be simply calibrated and corrected by multiplying the tested SNR by a correction coefficient, i.e., the coefficient 0.1 in Eq. (9) is corrected. Figure 14 displays the corrected results of the tested SNRs. As can be seen, the estimation errors of SNRs of weak sinusoidal and square-wave signals are within 2.5 dB.

To verify that the proposed technique has the ability to detect the frequency of weak signals with known SNR, a frequency test was implemented. The test frequency was from 0.3 to 2.4 MHz, with a step of 0.3 MHz. The SNR of the weak signal was -10 , -20 , and -30 dB. The tested DWEM values were corrected as shown in Fig. 14. The frequency test results of weak sinusoidal and square-wave signals are shown in Fig. 15. It can be observed that the frequency

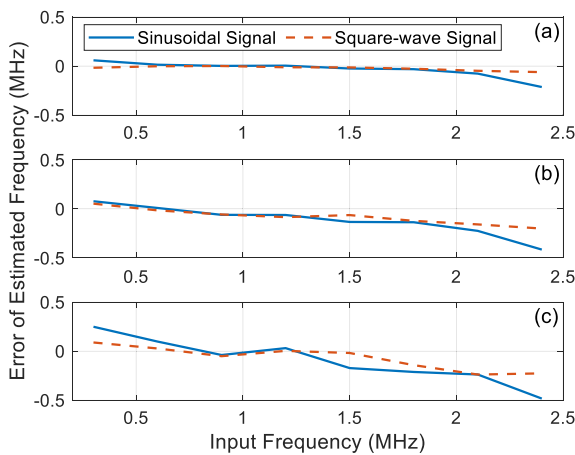


FIG. 15. Test results of frequency estimation with the SNR of (a) -10 dB, (b) -20 dB, and (c) -30 dB.

estimation is achievable by the proposed technique, and the estimation error is smaller in the situation of higher SNR. It is worth noting that the correction coefficient is related to the frequency of a weak signal. For accurate detection of weak signals with frequency variations over a large range, a series of tests can be conducted to obtain frequency related correction coefficients. Thus, a more accurate estimation of the SNR or frequency of the weak signal can be achieved, as the correction coefficient is selected due to the estimated frequency of the tested signal.

IV. CONCLUSION

In this article, a weak signal detection technique based on the DW test and one-bit sampling is proposed. The weak periodic signal is one-bit sampled using a CMP outside the FPGA and several SRs inside the FPGA. The DW test is performed on the one-bit data to detect weak sinusoidal or square-wave signals carried in the noise and to estimate the SNR or frequency of the weak signal, depending on the degree to which the randomness of the noise is affected. Simulation results demonstrate that the proposed technique can detect weak signals above -30 dB. In addition, the relationship between the DWEM, the frequency of the weak signals and the SNR is derived. The interferences of coherent sampling, noise bandwidth, and CMP threshold on the proposed technique are simulated and discussed. In the measured results, weak sinusoidal and square-wave signals above -30 dB are effectively detected, verifying the effectiveness of the proposed weak signal detection technique.

ACKNOWLEDGMENTS

This work was supported by the Startup Foundation for Introducing Talent at NUIST (Grant No. 1511132101014).

AUTHOR DECLARATIONS

Conflict of Interest

The authors have no conflicts to disclose.

Author Contributions

Xiru Zhao: Investigation (equal); Methodology (equal); Validation (lead); Writing – original draft (equal). **Jiadong Hu:** Funding acquisition (lead); Investigation (equal); Methodology (equal); Resources (equal); Validation (supporting); Writing – review & editing (lead). **Kenan Wu:** Software (lead); Writing – review & editing (supporting). **Haiyun Xia:** Resources (equal); Writing – review & editing (supporting). **Daihao Yu:** Validation (supporting); Writing – original draft (supporting).

DATA AVAILABILITY

The data that support the findings of this study are available within the article.

REFERENCES

- ¹J. Wang, L. Yang, L. Gao, and Q. Miao, "Current progress on weak signal detection," in *2013 International Conference on Quality, Reliability, Risk, Maintenance, and Safety Engineering (QR2MSE)* (IEEE, 2013), pp. 1812–1818.
- ²J. Hu, Z. Shen, S. Liu, and Q. An, "A field programmable gate array based high speed real-time weak periodic signal detection technique," *Rev. Sci. Instrum.* **92**, 024703 (2021).
- ³R. Wang, L. Chen, Y. Zhao, and G. Jin, "A high signal-to-noise ratio balanced detector system for 2 μm coherent wind lidar," *Rev. Sci. Instrum.* **91**, 073101 (2020).
- ⁴G. Duan, Y. Wang, Y. Zhang, S. Wu, and L. Lv, "A network model for detecting marine floating weak targets based on multimodal data fusion of radar echoes," *Sensors* **22**, 9163 (2022).
- ⁵M. Zhan, C. Zhao, K. Qin, P. Huang, M. Fang, and C. Zhao, "Subaperture key-stone transform matched filtering algorithm and its application for air moving target detection in an SBEWR system," *IEEE J. Sel. Top. Appl. Earth Observ. Remote Sens.* **16**, 2262–2274 (2023).
- ⁶H. Zhang, Z. Qin, Y. Zhang, D. Chen, J. Gen, and H. Qin, "A practical underwater information sensing system based on intermittent chaos under the background of Lévy noise," *EURASIP J. Wireless Commun. Networking* **2022**, 41.
- ⁷J. Yu, Q. Li, H. Li, Q. Wang, G. Zhou, D. He, S. Xu, Y. Xia, and Y. Huang, "High-precision light spot position detection in low SNR condition based on quadrant detector," *Appl. Sci.* **9**, 1299 (2019).
- ⁸X. Li, E. Leitinger, A. Venus, and F. Tufvesson, "Sequential detection and estimation of multipath channel parameters using belief propagation," *IEEE Trans. Wireless Commun.* **21**, 8385–8402 (2022).
- ⁹J. Tang, B. Shi, Z. Li, and Y. Li, "Weak fault feature extraction method based on compound tri-stable stochastic resonance," *Chin. J. Phys.* **66**, 50–59 (2020).
- ¹⁰Z. Huo, Y. Zhang, P. Francq, L. Shu, and J. Huang, "Incipient fault diagnosis of roller bearing using optimized wavelet transform based multi-speed vibration signatures," *IEEE Access* **5**, 19442–19456 (2017).
- ¹¹T. Han, L. Ding, D. Qi, C. Li, Z. Fu, and W. Chen, "Compound faults diagnosis method for wind turbine mainshaft bearing with Teager and second-order stochastic resonance," *Measurement* **202**, 111931 (2022).
- ¹²P. Rudnick, "The detection of weak signals by correlation methods," *J. Appl. Phys.* **24**, 128–131 (1953).
- ¹³O. Sharifi-Tehrani and M. F. Sabahi, "Eigen analysis of flipped Toeplitz covariance matrix for very low SNR sinusoidal signals detection and estimation," *Digital Signal Process.* **129**, 103677 (2022).
- ¹⁴H. Xu, H. Pan, J. Zheng, Q. Liu, and J. Tong, "Dynamic penalty adaptive matrix machine for the intelligent detection of unbalanced faults in roller bearing," *Knowledge-Based Syst.* **247**, 108779 (2022).
- ¹⁵X. Guo, H. Li, Y. Chen, and W. Sun, "A low-computing-complexity touch signal detection method and analog front-end circuits based on cross-correlation technology for large-size touch panel," *Sensors* **22**, 4354 (2022).
- ¹⁶X. Chen, M. Wei, K. Chen, and S. Li, "Research on weak signal detection of integral average digital lock-in amplifier," *Meas. Sci. Technol.* **32**, 105905 (2021).
- ¹⁷M. Saritha, M. Lavanya, G. Ajitha, M. N. Reddy, P. Annapurna, M. Sreevani, S. Swathi, S. Sushma, and V. Vijay, "A VLSI design of clock gated technique based ADC lock-in amplifier," *Int. J. Syst. Assur. Eng. Manage.* **13**, 2743–2750 (2022).
- ¹⁸M. Fan, T. Lan, G. Li, and L. Ling, "Suppression of odd harmonic interference in a fast digital lock-in amplifier based on square wave signal," *IEEE Trans. Instrum. Meas.* **72**, 2003208 (2023).
- ¹⁹L. Zhao, H. Tao, W. Chen, and D. Song, "Maneuvering target detection based on subspace subaperture joint coherent integration," *Remote Sens.* **13**, 1948 (2021).
- ²⁰L. Lin, Z. Cheng, and Z. He, "Coherent detection and parameter estimation for ground moving target based on MLRT-IDCFT," *Digital Signal Process.* **120**, 103259 (2022).
- ²¹S. Liu, Y. Sun, and Y. Kang, "A novel E-exponential stochastic resonance model and weak signal detection method for steel wire rope," *IEEE Trans. Ind. Electron.* **69**, 7428–7440 (2021).
- ²²Z. Qiao, Y. Lei, and N. Li, "Applications of stochastic resonance to machinery fault detection: A review and tutorial," *Mech. Syst. Signal Process.* **122**, 502–536 (2019).
- ²³M. Li, P. Shi, W. Zhang, and D. Han, "Stochastic resonance in a high-dimensional space coupled bistable system and its application," *Appl. Math. Modell.* **113**, 160–174 (2023).
- ²⁴G. Li, J. Cui, and H. Yang, "A new detecting method for underwater acoustic weak signal based on differential double coupling oscillator," *IEEE Access* **9**, 18842–18854 (2021).
- ²⁵G. Wang, L. Yang, X. Zhan, A. Li, and Y. Jia, "Chaotic resonance in Izhikevich neural network motifs under electromagnetic induction," *Nonlinear Dyn.* **107**, 3945–3962 (2022).
- ²⁶S. Cao, H. Li, K. Zhang, C. Yang, F. Sun, and Z. Wang, "An improved chaotic recognition method for weak signal frequency and its application to fault diagnosis of planetary gearboxes," *Meas. Sci. Technol.* **33**, 105113 (2022).
- ²⁷J. Gu, Y. Peng, H. Lu, X. Chang, and G. Chen, "A novel fault diagnosis method of rotating machinery via VMD, CWT and improved CNN," *Measurement* **200**, 111635 (2022).
- ²⁸S. Jiao, R. Gao, D. Zhang, and C. Wang, "A novel method for UWB weak signal detection based on stochastic resonance and wavelet transform," *Chin. J. Phys.* **76**, 79–93 (2022).
- ²⁹J. Wang, C. Ye, M. Jiang, F. Zhang, and Q. Sui, "SWT-KELM-based rolling bearing fault diagnosis method under noise conditions with different SNRs," *Meas. Sci. Technol.* **34**, 015007 (2022).
- ³⁰R. Benzi, A. Sutera, and A. Vulpiani, "The mechanism of stochastic resonance," *J. Phys. A: Math. Gen.* **14**, L453 (1981).
- ³¹R. Benzi, G. Parisi, A. Sutera, and A. Vulpiani, "Stochastic resonance in climatic change," *Tellus B* **34**, 10–16 (2012).
- ³²R. Benzi, G. Parisi, A. Sutera, and A. Vulpiani, "A theory of stochastic resonance in climatic change," *SIAM J. Appl. Math.* **43**, 565–578 (1983).
- ³³S. Lu, Q. He, and J. Wang, "A review of stochastic resonance in rotating machine fault detection," *Mech. Syst. Signal Process.* **116**, 230–260 (2019).
- ³⁴Q. Wang, Y. Yang, and X. Zhang, "Weak signal detection based on Mathieu-Duffing oscillator with time-delay feedback and multiplicative noise," *Chaos, Solitons Fractals* **137**, 109832 (2020).
- ³⁵J. Durbin and G. S. Watson, "Testing for serial correlation in least squares regression. I," *Biometrika* **37**, 409–428 (1950).
- ³⁶J. Durbin and G. S. Watson, "Testing for serial correlation in least squares regression. II," *Biometrika* **38**, 159–178 (1951).
- ³⁷S. S. Uyanto, "Power comparisons of five most commonly used autocorrelation tests," *Pak. J. Stat. Oper. Res.* **16**, 119–130 (2020).
- ³⁸T. S. Breusch, "Testing for autocorrelation in dynamic linear models," *Aust. Econ. Pap.* **17**, 334–355 (1978).
- ³⁹L. G. Godfrey, "Testing against general autoregressive and moving average error models when the regressors include lagged dependent variables," *Econometrica* **46**, 1293–1301 (1978).
- ⁴⁰H. Hassani and M. R. Yeganegi, "Selecting optimal lag order in Ljung–Box test," *Physica A* **541**, 123700 (2020).
- ⁴¹S. Sharma, V. Bhatia, K. Deka, and A. Gupta, "Sparsity-based monobit UWB receiver under impulse noise environments," *IEEE Wireless Commun. Lett.* **8**, 849–852 (2019).
- ⁴²Y. Chen, "Spatial autocorrelation approaches to testing residuals from least squares regression," *PLoS One* **11**, e0146865 (2016).
- ⁴³Texas Instruments, Inc., TLV3604DCR: High-Speed RRI comparator with LVDS Outputs, <https://www.ti.com/lit/ds/symlink/tlv3604.pdf>, 2024.
- ⁴⁴AMD XLINX, Inc., XC7K325T-2FFG900I: DC and AC Switching Characteristics, <https://docs.xilinx.com/v/u/en-US/7-series-product-selection-guide>, 2024.